

**CALL #:** [http://sfx.fcla.edu/ucf?url\\_ver=Z39.88-2004&ctx\\_ver=Z39.88-2...](http://sfx.fcla.edu/ucf?url_ver=Z39.88-2004&ctx_ver=Z39.88-2...)

**LOCATION:** **FTU :: Electronic :: World Scientific Journals:Full Text**

**TYPE:** Article CC:CCG

**JOURNAL TITLE:** International journal of structural stability and dynamics [electronic resource].

**USER JOURNAL TITLE:** International Journal of Structural Stability and Dynamics

**FTU CATALOG TITLE:** International journal of structural stability and dynamics

**ARTICLE TITLE:** PHYSICAL PARAMETER IDENTIFICATION OF AN RC FRAME STRUCTURE ON ELASTIC FOUNDATION

**ARTICLE AUTHOR:**

**VOLUME:** 9

**ISSUE:** 4

**MONTH:** December

**YEAR:** 2009

**PAGES:** 627-648

**ISSN:** 0219-4554

**OCLC #:**

**CROSS REFERENCE ID:** [TN:198633][ODYSSEY:129.25.131.206/DXU]

**VERIFIED:**

**BORROWER:** **DXU :: Hagerty Library**

**PATRON:** **Yun Zhou**

**PATRON ID:** yz79

**PATRON ADDRESS:**

**PATRON PHONE:**

**PATRON FAX:**

**PATRON E-MAIL:**

**PATRON DEPT:**

**PATRON STATUS:**

**PATRON NOTES:**

## PHYSICAL PARAMETER IDENTIFICATION OF AN RC FRAME STRUCTURE ON ELASTIC FOUNDATION

YUN ZHOU and WEI-JIAN YI\*

*College of Civil Engineering, Hunan University, Changsha  
Hunan 410082, P. R. China  
\*wjyi@hnu.cn*

Received 2 February 2008

Accepted 4 December 2008

In this paper, the simple genetic algorithm (SGA) is improved by combining with the simulated annealing algorithm (SAA) for the parameter identification of a reinforced concrete (RC) frame on elastic foundation. SGA adopts parallel search strategy, which is based on the concept of “survival of the fittest” in optimization while SAA adopts a serial form and the process is endowed with time-variant probable jumping property so that local optimization could be prevented. The global searching ability is developed by combining the two methods and the new algorithm is named genetic annealing hybrid algorithm (GAHA). Modal experiments were carried out on a four-storey RC frame structural model with isolated embedded footings in laboratory. The measured natural frequencies and mode shapes have been utilized to identify the physical parameters of the frame by the proposed method. Four cases of concrete elastic modulus and foundation dynamic shear modulus are identified, and the results are compared with the usual sensitivity methods (SM). By model updating, the results show that the elastic modulus of concrete increases with respect to the storey. The identified elastic modulus of the concrete is generally larger than that found by compressive testing because the dynamic modulus of concrete is larger than the static modulus of concrete. The identified soil dynamic shear modulus also increases with the storey since the soil property depends on the pressure exerted on the soil. It is also shown that the identified results by GAHA are better than that of SM.

*Keywords:* Parameter identification; modal experiment; reinforced concrete frame structure; soil foundation; genetic annealing hybrid algorithm; sensitivity method; model updating.

### 1. Introduction

Experimental modal analysis based structural physical parameter identification methodologies have been widely studied in the last two decades. Friswell and Mottershead<sup>1</sup> gave extensive reviews of various model-updating methods that have been developed. Comprehensive literature reviews on vibration based structural identification and model updating within the context of civil engineering can be found in Refs. 2 and 3. The natural frequencies and mode shapes by dynamic measurement of the structures are often influenced by soil–structure interaction (SSI). Usually, the field-measured natural frequencies of a structure are lower than the

calculated results by finite element method analysis, because the fully rigid constraints supposed by theoretical analysis do not exist in practice, in which SSI inevitably causes the decrease in static and dynamic stiffness of a structure.

Research on SSI has made great progress on theoretical methods, but it has been blocked from further developments due to the lack of experimental and real data. The dynamic experimental testing can reflect the real structural dynamic properties, and the SSI may be the most important factor that should be carefully considered in structural dynamic analysis. Some researchers studied the influence of SSI on the identification of structural parameters. There are also a few experimental tests on engineering structures to validate the effects of SSI. Whitman *et al.*<sup>4</sup> established a dynamic equilibrium equation to identify the horizontal and vertical impedance of the foundation. Wong and Trifuriac<sup>5</sup> found significant changes in natural frequencies identified from the responses of a seven-storey reinforced concrete (RC) hotel building in Vn Nuys, California during 12 seismic events. Hans *et al.*<sup>6</sup> conducted ambient vibration, harmonic vibration, and shock loading tests on five decommissioned buildings. After Northridge earthquake, Chassiakos *et al.*<sup>7</sup> strengthened the Long Beach Public Safety Building by shear walls storey by storey and measured different modal characters of the building. Luco and Barros<sup>8</sup> identified the structure and foundation parameters from forced vibration testing on Hualien containment model in Taiwan.

Many traditional optimization methods are gradient-based methods. This method is simple and effective for some optimization problems but it sometimes leads to a local minimum. Genetic algorithm (GA) is a global search method. Over the past three decades, the algorithm has been widely used in parameter identification and damage diagnosis. GA is based on Darwin's theory of natural selection (i.e. the "survival of the fittest") and John Holland brought it forward in 1970s. The key steps in GA are encoding, selection, crossover, and mutation. In recent years, many efforts have been made by researchers to optimize the configuration of GA and to incorporate local search algorithms so as to improve its performance continuously.

Friswell *et al.*<sup>9</sup> used a combined GA and eigensensitivity method to identify the location and magnitude of damage from measured vibration data, the GA is used to identify the damage location and the eigensensitivity is used to identify the damage extent. Yi and Liu<sup>10</sup> developed some improved strategies, such as multi-parents crossover and fine-tuning of variables, to detect the damage of a fixed-end beam. Hao and Xia<sup>11</sup> used real number encoding to identify the structural damage by minimizing the objective function, considering different criteria. Au *et al.*<sup>12</sup> used an elemental energy quotient difference to locate the damage domain and to quantify the damage extent by minimizing the errors between the measured data and numerical results. Lu and Tu<sup>13</sup> presented a real-coding GA-based model updating approach for global model updating based on dynamic measurement data, an eigensensitivity method is used to further fine-tune the GA updated results in case the sensitivity problem arises due to restricted measurement information. It combines the virtues of

the two algorithms. Perera and Torres<sup>14</sup> proposed nonclassical optimization approach involving the use of GA to localized damage areas of the structure. GA yields a suitable damage location and severity detection while introducing numerous advantages when compared to classical methods. Perry *et al.*<sup>15</sup> proposed a modified GA strategy to improve the accuracy and computational time for parameter identification of multiple degree-of-freedom structural systems, in which the strategy includes multiple populations or “species,” a search space reduction procedure and new operators designed to provide a robust and reliable identification. Sahoo and Maity<sup>16</sup> indicated that the artificial neural network has no specific recommendation on suitable design of network for different structures. The parameters are selected by trial and error and a hybrid neuro-GA is proposed in order to design the neural network for different types of structures.

Simulated annealing algorithm (SAA) is another optimization algorithm, it is good at hill climbing for optimum solutions, but the convergence speed may be slow. Balling<sup>17</sup> used simulated annealing strategy to develop a discrete optimization method for design of three-dimensional steel frames. Levin and Lieven<sup>18</sup> compared various implementations of the two algorithms for model updating purposes, and then developed a new variant of SA method. They found that the new method could be the most effective of all optimization algorithms. Tzan and Pantelides<sup>19</sup> presented an annealing method to obtain the optimal design of structural systems, the method required lesser iterations to converge as compared to other simulated annealing methods. He and Hwang<sup>20</sup> combined the real-parameter GA with SA to detect damage in a simply supported sector of a spherical laminate shell. The proposed method could predict the locations precisely, thereby demonstrating that the SAA could be combined with other algorithms and is good for local hill climbing.

In this paper, GA is improved by combining with the SAA. The two algorithms are combined in a serial form, called genetic annealing hybrid algorithm (GAHA). A four-storey RC frame structure was built on the soft soil for the modal experimental tests. When the frame structure was constructed storey by storey, the hammer impact modal experiments were conducted and hence we have four cases of modal tests. Based on the sound numerical structure and foundation models, the proposed GAHA was used to identify the elastic modulus of the concrete and dynamic shear modulus of the soil of foundation, and the changes of the modulus were obtained. GAHA is found to have a good behavior when the identified results were compared with those identified by the sensitivity method (SM).

## 2. Genetic Annealing Hybrid Algorithm (GAHA)

### 2.1. Genetic algorithm (GA)

GA adopts the mechanism of biological evolution to perform optimization. It is based on the strategy of “survival of the fittest.” GA can search the whole solution space to obtain the global optimal solution. The chromosomes refer to a candidate solution.

The individual chromosome is composed of a number of “genes.” Different numbers of genes represent different variables. Fitness is the objective function value of the candidate solution. GA starts with a random population of  $n$  chromosomes. The initial population evolves throughout generations until convergence to a desired solution. The main process of GA includes reproduction, crossover, and mutation. Reproduction is a process to select the best individual in population based on their fitness, in which the generation has more chances to reproduce the chromosomes in the next generation. Crossover is very important to randomly select father generation and to change a part of chromosomes in the gene to produce two new offsprings. It reflects the principle of “information changes.” Mutation is to change randomly one or more of the genes in chromosomes in order to introduce new characteristics into the population.

Following the aforementioned three main steps, the father individuals produce a new generation, the process can be called simple genetic algorithm (SGA). Some researchers proved that SGA might not reach the global optimum. In addition, it spends much computational time in the encoding and decoding process and it lacks the “hill-climbing ability.”<sup>15</sup> Another two problems exist in SGA, that is “cheating problem” and “premature problem,” and they can hardly be solved. Therefore, SGA needs to be improved. Some researchers proposed the hybrid GA that improves GA by merging it into another algorithm.

## 2.2. Simulated annealing algorithm (SAA)

SAA is another optimization algorithm. It is good at hill climbing but it lacks computational efficiency. SAA belongs to a nonlinear inversion algorithm. The basic idea comes from the thermodynamic cooling process. Many materials have one crystalline low-energy state and multiple glassy high-energy states. Annealing is a method of finding the lowest energy state from all of the possible stable states.<sup>18</sup> The annealing process consists of heating the substance until it is molten, and then slowly decreasing the temperature. The substance is allowed to reach thermal equilibrium at each temperature. If the temperature decreases sufficiently slowly, the annealing process picks out the global minimum energy state from the infinite number of other possible states.<sup>18</sup>

In 1953, Metropolis co-authored proposed an “importance-sampling method,” they assumed the particles in the solid establish in initial status  $i$ , the energy status is set as  $E_i$ . Then the perturbation method was used to make the particle change the positions randomly, a new status is obtained with the energy status  $E_j$ . If  $E_j < E_i$ , the new status can be set as “important status,” and if  $E_j > E_i$ , according to the probability of the solid exists in some status it is determined whether the new status is accepted as an “important status.” The probability of the solid in status  $i$  or in status  $j$  is equal to the ratio of Boltzman gene, as shown in Eq. (1):

$$r = \exp\left(\frac{E_i - E_j}{kT}\right) \quad (1)$$

in which  $T$  is the temperature and  $r$  is a number less than 1. Another random number  $\xi$  in  $[0, 1)$  will be randomly produced. If  $r > \xi$ , the new status will be set as an important status, otherwise it will be abandoned. If the new status  $j$  is in the "important status," status  $j$  will replace status  $i$  as the current status, otherwise status  $i$  is the current status. After a large scale transferring process of the particles, the system will get into a lower energy equilibrium status. In a high temperature, the new status have larger differences with the current status and it can be accepted as an "important status," but in a low temperature the new status have little differences with the current status. It seems like there is thermodynamic influence on different temperature status. The aforementioned description is the main idea of Metropolis criterion.<sup>21</sup>

In 1982, Kirkpatrick<sup>21,22</sup> proposed SAA. Under some initialization temperatures, with the decreasing of the temperature, the probabilistic jumping property is endowed to search the global optimum solution in the objective function. The optimization process based on the Metropolis criterion has local hill-climbing property, as shown in Fig. 1. When the solution value is trapped in the local optimum point A, the probabilistic jumping property can make the solution jump over the point B and to reach the global optimum point C. So the local minimum point can be prevented otherwise it overcomes the shortcomings of the searching process that highly depends on the initial value. The process goes into cycles for several times and the system will reach equilibrium status, which satisfies a normal distribution.

**2.3. Genetic annealing hybrid algorithm (GAHA)**

GA and SAA are both probabilistic searching algorithms, which are capable of finding global optimum results in complicated optimization problems. Both are derived from analogies with natural phenomena. SAA is like a thermodynamic cooling process and GA simulates the biological evolution process.<sup>18</sup> Their shortcomings can be overcome when they are combined together. The GAHA is shown in

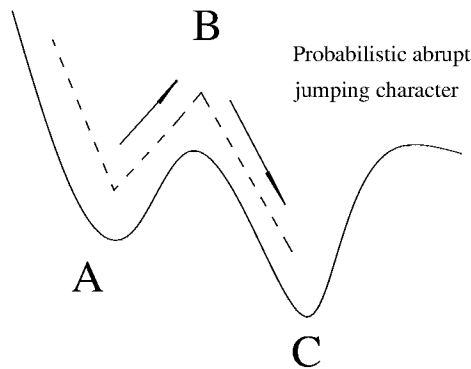


Fig. 1. Probabilistic abrupt jumping character of SA.

Fig. 2. SAA in GAHA adopts a serial form and the process is endowed with time-variety probabilistic jumping property so that the local minimum is prevented and the global optimum could be obtained. SAA can prevent the weakness in GA and GA reduces the time cost in SAA. The search ability can be highly improved and the initial parameters' selection is not strict any more.

In this serial form, the initial value of SAA comes from evolution results of GA. By using the Metropolis criterion and annealing process of SAA, the populations become the initial values of GA. SAA in high temperature is helpful to population's large scale transferring. When SAA is in low temperature the mutation in GA is helpful to search the local optimum results.<sup>22</sup> In this study, GAHA is used to identify physical parameter of a four-storey RC frame structure on elastic foundation.

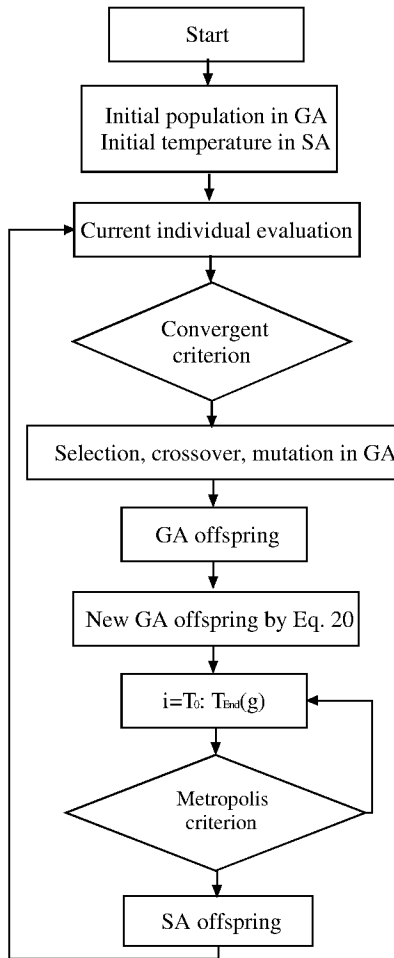


Fig. 2. Flow chart of GASA.

### 3. Sensitivity Method (SM)

In order to compare with GAHA, the traditional simple SM is used for comparison. In SM, the eigen-values and mode shape vectors are expanded by the first-order Taylor series as follows:

$$\begin{pmatrix} \lambda(P) \\ \phi(P) \end{pmatrix} = \begin{pmatrix} \lambda(P) \\ \phi(P) \end{pmatrix}_{\{P\}=\{P\}_a} + [S](\{P\} - \{P\}_a), \tag{2}$$

where  $\lambda(P)$ ,  $\phi(P)$  is the vector composed of the natural frequencies and mode shapes extracted from experimental measurements, respectively.  $\lambda(P)_{\{P\}=\{P\}_a}$ ,  $\phi(P)_{\{P\}=\{P\}_a}$  is the vector of the corresponding natural frequencies and mode shapes determined by numerical analysis when  $\{P\} = \{P\}_a$ . The sensitivity-based matrix  $[S]$  can be solved by numerical perturbation method

$$[S] = \begin{bmatrix} S_\lambda \\ S_\phi \end{bmatrix} = \begin{bmatrix} \frac{\partial \lambda}{\partial P} \\ \frac{\partial \phi}{\partial P} \end{bmatrix}. \tag{3}$$

Equation (2) can be rewritten as follows:

$$\{\Delta P\} = \{P\} - \{P\}_a = [S]^+ \left( \begin{pmatrix} \lambda(P) \\ \phi(P) \end{pmatrix}_{\{P\}=\{P\}_a} - \begin{pmatrix} \lambda(P) \\ \phi(P) \end{pmatrix} \right). \tag{4}$$

Equation (4) is determined, over-determined or under-determined depending on whether the number of available responses  $N$  is equal to, larger than or smaller than the number of unknown parameters  $M$ . The parameter modification  $\{\Delta P\}$  can be solved using the pseudo-inverse technique.  $[S]^+$  is the pseudo-inverse matrix of sensitivity matrix  $[S]$  and is given by Eq. (5),<sup>23</sup>

$$[S]^+ = \begin{cases} [S]^{-1} & N = M \\ ([S]^T [S])^{-1} [S]^T & N > M \\ [S]^T ([S][S]^T)^{-1} & N < M. \end{cases} \tag{5}$$

The identified physical parameters by SM are used to compare with the results identified by GAHA.

## 4. Modal Experiments of RC Frame Model on Elastic Foundation

### 4.1. Introduction of the experimental model

The experiment was carried out on the soil pit in the Structural Engineering Laboratory of Hunan University. The structural model, as shown in Fig. 3, is a four-storey RC frame. Beneath each column there is an independent embedded footing with a plan dimension of  $0.6 \times 0.6$  m, Reinforcement details of the beam and column elements are given in Table 1. The floor slab is 30 mm thick and reinforced nominally



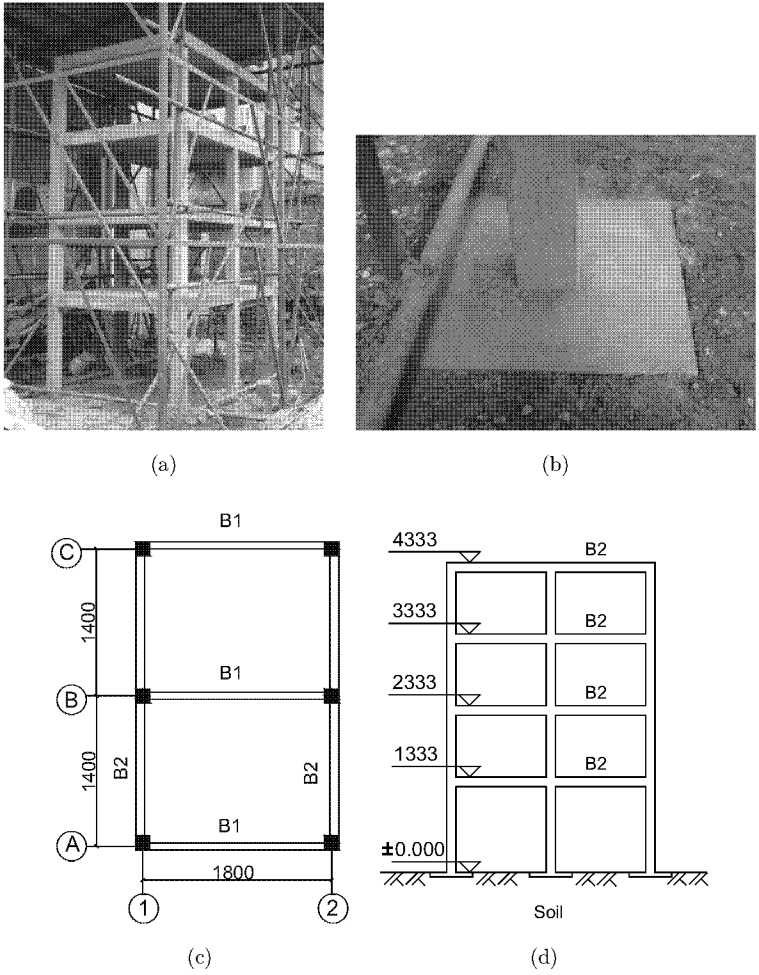


Fig. 3. Frame configuration: (a) photo of model frame structure; (b) photo of embedded isolated footing; (c) plane view and dimensions; (d) elevation of North–South frames (all dimensions are in mm).

Table 1. Reinforcement data of frame elements.

Description	Dimensions (mm)	Reinforcement	
		Longitudinal	Transverse
Column	133 × 133	4-Φ8	Φ3@30 mm
Beams B1	67 × 167	3-Φ8 top	Φ3@30 mm
		3-Φ8 bottom	
Beams B2	83 × 133	3-Φ8 top	Φ3@30 mm
		2-Φ8 bottom	

with 3 mm diameter bars at a spacing of 30 mm in each direction for both positive and negative bending as needed. The yield strength of the reinforcing bars is 235 MPa. The pit was filled with 1.2 m clay soil which was compacted at 20–30 cm intervals. The density of the clay is 1965.2 kg/m<sup>3</sup> with a moisture content of 18.85%. Bearing plate experiments indicate that the static elastic modulus of the filled powder clay is 48.1 MPa. A three-dimensional soil pressure system TSZ-30B (which is a strain-controlled three-axis pressure system) was used to measure the shear strength of the soil. Based on recorded measurements of four soil samples under different uniform confined pressures, the characteristics of the soil are:  $C = 55.8$  kPa and  $\varphi = 8.5^\circ$  based on the Mohr–Coulomb criterion.

The dynamic characteristics of the soil foundation were measured by the impulse excitation method.<sup>24</sup> Low ratios of signal to noise could result in measurement errors in the Rayleigh wave identification. However, prior knowledge of the dynamic properties of soil was utilized to determine the range of frequency, in which the Rayleigh wave could be identified. Three vertical accelerometers were placed 3 m apart in the direction of the transmitting wave as shown in Fig. 4. The hammer was used to excite a wide-band frequency response in the soil. Transducers were employed to intercept the Rayleigh waves. If the frequency of the Rayleigh wave is  $f_R$ , the time difference for the wave to reach adjacent transducers is  $\Delta t$  and the phase difference is  $\Delta\varphi$ , then the transmitting velocity of the Rayleigh wave is given by

$$v_R = \frac{\Delta x}{\Delta t} = 2\pi f_R \cdot \frac{\Delta x}{\Delta\varphi}. \tag{6}$$

According to the elastic wave theory, the relationship between the shear wave velocity and the Rayleigh wave velocity is

$$v_s = \frac{1 + \nu}{0.87 + 1.12 \nu} \cdot v_R. \tag{7}$$

The dynamic shear modulus  $G_d$  and dynamic elastic modulus  $E_d$  of the soil are defined as:

$$G_d = \rho v_s^2, \tag{8}$$

$$E_d = 2(1 + \nu)\rho v_s^2, \tag{9}$$

where  $\rho$  is the density of the soil and  $\nu$  the damping ratio of the soil. By assuming a damping ratio  $\nu = 0.3$ , the soil characteristics shown in Table 2 were obtained. The

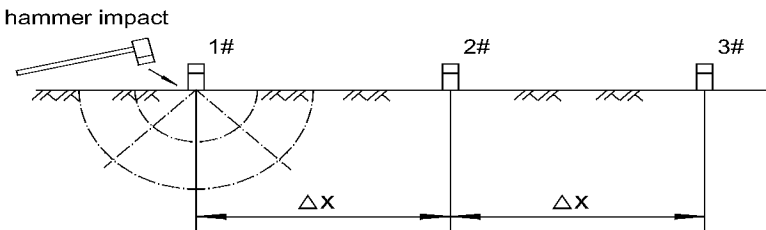


Fig. 4. Rayleigh wave measurement by hammer impact method.

Table 2. Dynamic properties of soil-foundation system.

Properties	Values
Rayleigh wave velocity, $v_R$	145.54 m/s
Shear wave velocity, $v_s$	156.88 m/s
Dynamic shear modulus, $G_d$	$4.837 \times 10^7$ N/m <sup>2</sup>
Dynamic elastic modulus, $E_d$	$1.258 \times 10^8$ N/m

elastic modulus of concrete  $E_c$  was evaluated in accordance with the empirical expression given by<sup>25</sup>

$$E_c = \frac{100}{2.2 + 34.7/\bar{f}_{cu}}. \tag{10}$$

In the above expression,  $\bar{f}_{cu}$  is the compressive strength obtained from testing 150 mm cubes. In this study, modal experiments were carried out respectively after the first, the second, the third, and the fourth storey were built. Therefore, we have four groups of modal experiments corresponding to different construction stages. They are designated as Case I, Case II, Case III, and Case IV and are shown in Fig. 5. The four groups of elastic modulus are listed in Table 3.

**4.2. Numerical model of frame structure on elastic foundation**

The dynamic impedance function proposed by Pais and Kausel<sup>26</sup> is used in the theoretical model of the embedded foundation slab. Generally the dynamic impedance function of the foundation is a function of frequency and can be expressed by

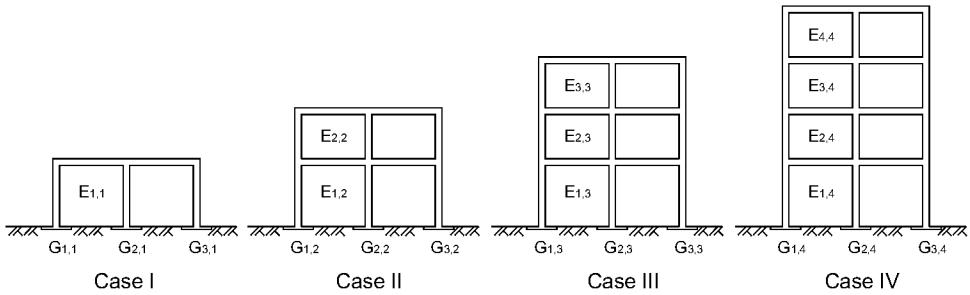


Fig. 5. Four cases of modal experiments. (Four cases of modal experiments when finish concrete casting every storey. In  $E_{i,j}$  and  $G_{i,j}$ ,  $i$  denotes the number of storey, and  $j$  denotes the number of case).

Table 3. Elastic modulus of the concrete ( $\times 10^7$  kN/m<sup>2</sup>).

Finish casting	First storey	Second storey	Third storey	Fourth storey
Case I	2.526	/	/	/
Case II	2.979	2.161	/	/
Case III	3.020	2.881	2.132	/
Case IV	3.456	3.329	3.364	3.085

$a_0 = \omega B/V_s$ . The horizontal, rocking, and coupled horizontal-rocking impedance functions are given by

$$K_{Hx}^d = K_{Hx}^s(G, B, v, L, e)(1.0 + ia_0c), \tag{11}$$

$$K_{Rx}^d = K_{Rx}^s(G, B, v, L, e, a_0)(k + ia_0c), \tag{12}$$

$$\bar{K}_{HR}^d = \frac{\left(\frac{e}{B}\right)\bar{K}_{Hx}^d}{3}, \tag{13}$$

where  $K^s$  is defined as the static stiffness of the foundation,  $\omega$  the natural circular frequency,  $L$  half the length of the foundation,  $B$  half of the width of the foundation,  $G$  the dynamic shear modulus of the soil,  $e$  the embedded depth of the slab,  $V_s$  the shear wave velocity,  $k$  the dynamic stiffness of the foundation, and  $c$  the damping coefficient of the foundation. The stiffness item in impedance function is the function of dynamic shear modulus, which is set as quantity in physical parameter identification.

Generally, the stiffness items in the equation of motion should be modified by adding the corresponding impedance function considering the influence of the foundation. Herein the added impedance items can be expressed as:

$$[\bar{k}] = \begin{bmatrix} K_{Hx} & K_{HR} \\ K_{HR} & K_{Rx} \end{bmatrix} \tag{14}$$

in which  $K_{Hx}$  is the horizontal impedance,  $K_{HR}$  the rocking impedance, and  $K_{HR}$  the horizontal rocking coupling impedance.

The simplest analytical model is the “shear-type” model, in which the bending deformation of beams and the axial deformation in all members are neglected. An accurate model in finite element method of frame structures includes the bending and axial deformations in all members. Herein, the “bending-shear” model is employed for the modal analysis, in which the bending deformation in all members is considered but the axial deformation is neglected. The results calculated with this model are close to the measured results, as shown in Table 4. The masses of the floors are concentrated at the corresponding floor beam. In order to account for the stiffness effect of the floor, the flexural stiffness of the edge beam is modified to  $1.5E_cI_b$ , as recommended in the Chinese Code.<sup>25</sup> Note that  $E_c$  is the elastic modulus of concrete and  $I_b$  the moment of inertia of a beam. Therefore, the flexural stiffness of the beams and columns in the planar frame are  $3E_cI_b$  and  $2E_cI_c$ , in which  $I_c$  is the moment of

Table 4. Comparison of different model results with the measured results.

Model selection	Frequency (Hz)				MAC			
	1st	2nd	3rd	4th	MAC <sub>1</sub>	MAC <sub>2</sub>	MAC <sub>3</sub>	MAC <sub>4</sub>
Measured results	7.7	25.9	50.8	79.5	/	/	/	/
Complete DOFs model	8.09	27.33	50.16	73.98	0.9935	0.9783	0.9870	0.9901
Bending shear condensing model	7.55	24.55	45.80	70.13	0.9981	0.9947	0.9982	0.9960

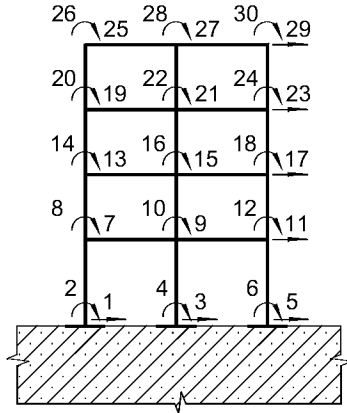


Fig. 6. Original finite element model of frame structure.

inertia of one column. Take Case IV as an example. The original structure have 24 degree-of-freedom (DOFs) as shown in Fig. 6, and it is further reduced to four by static condensation as shown in Fig. 7. There are six boundary DOFs that account for the contribution of each foundation. Therefore, the whole soil-structure coupled structure is modeled as a 10-DOFs system as shown in Fig. 7. There are seven unknown parameters including elastic modulus of concrete in each storey,  $E_1, E_2, E_3,$  and  $E_4$ , and the dynamic shear modulus of the isolated footing,  $G_1, G_2,$  and  $G_3$ . The lumped mass matrix is used.

**4.3. Modal experiments on frame structure**

PCB hammer 086D20 with a black cap (with sensitivity of 0.23 mv/N, black cap is the hardest) and 626A12 PCB accelerometers (with sensitivity of 100 mv/g) were used to excite and intercept the dynamic signals on the superstructure of the RC frame. The excitation and response signals were collected by the ABAQUS signal analyzer, and then analyzed with complex polynomial method by Me'Scope software.

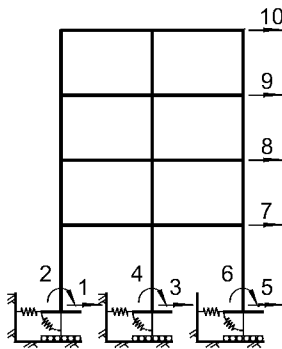


Fig. 7. Condensed finite element model of frame structure and soil coupled system.

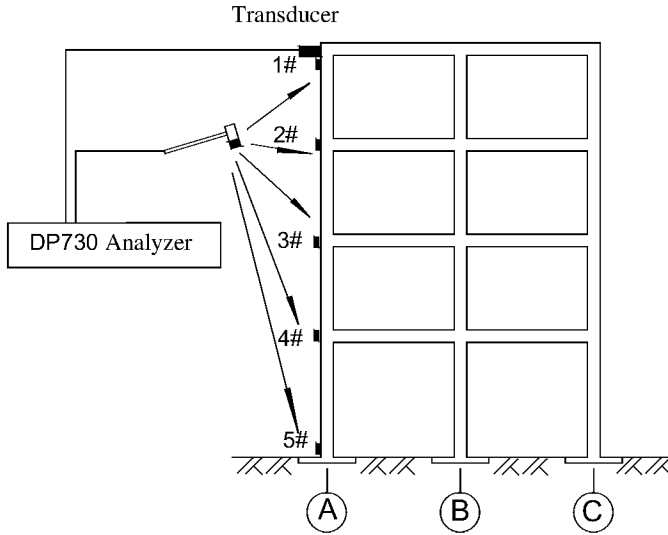


Fig. 8. Hammer impact modal experiment on frame structure in Case IV.

The accelerometer was placed on the top storey of the frame, as shown in Case IV in Fig. 8. The measured input and output signals in Case IV are shown in Fig. 9. The modal experiment in each case was carried out with multi-input and single-output method. Measurement direction was in the ② axis in Fig. 3(c). The transfer functions in different cases are shown in Fig. 10. The translational modes in this direction and torsional modes can be excited. As shown in Fig. 10, for Case IV, the eight peaks of the transfer function correspond to eight modes, in which the odd number corresponds to the translational mode and the even number represents the torsional mode due to the signal exciting and picking up were located along the symmetry axis. The natural frequencies and damping ratios obtained from modal analysis are listed in Table 5. The measured and identified vibration mode shapes will be given

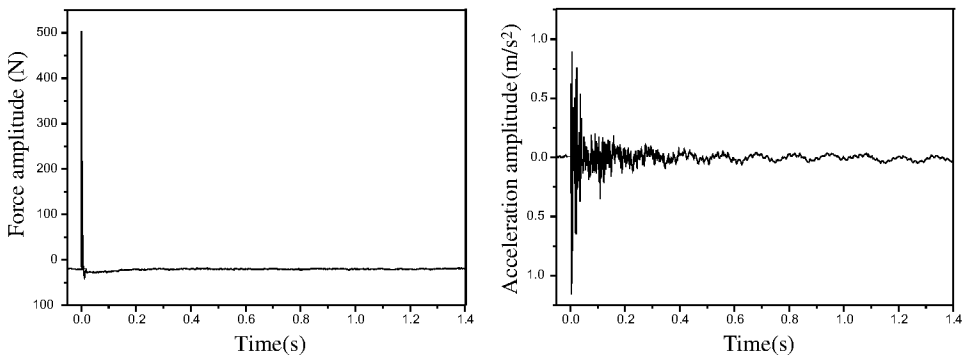


Fig. 9. Force and response time curves in Case IV.

Table 5. The modal experiment results of four cases.

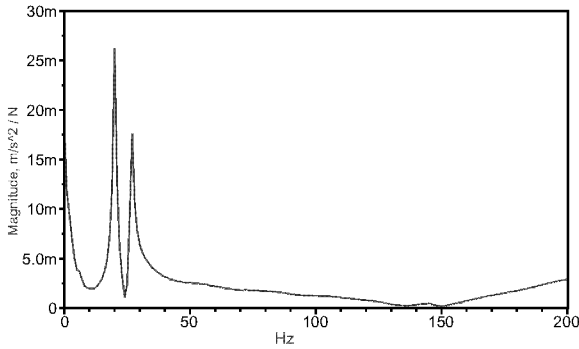
Case	I		II		III			IV		
Modal number	1st	1st	2nd	1st	2nd	3rd	1st	2nd	3rd	4th
Natural frequency (Hz)	20.1	13.4	51.2	9.86	34.1	69.3	7.67	26.1	50.6	79.3
Damping ratio (%)	2.68	2.01	1.82	2.28	1.81	1.18	1.57	2.10	0.89	1.14

in the following section. Note that only the translational modes are used in the identification.

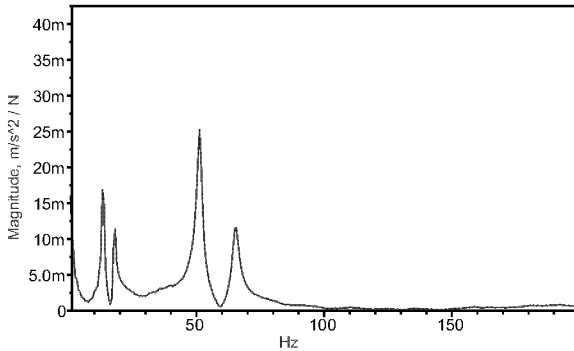
### 5. Physical Parameter Identification Based on GAHA

#### 5.1. Objective criterion and initial parameter selection

The common optimization approach in model updating is to update the physical parameters of the analytical model so that the differences between the analytical vibration data after updating and the measured vibration data are minimized. Measurement noise and analytical structural model errors are important factors

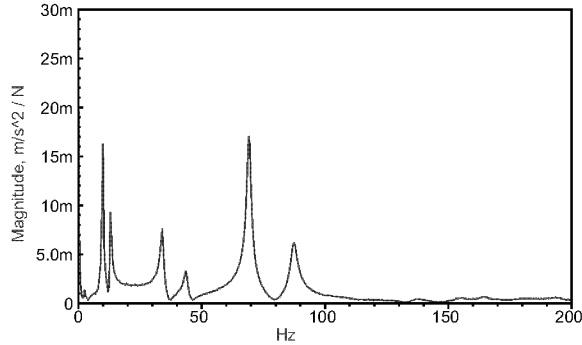


(a) Case I

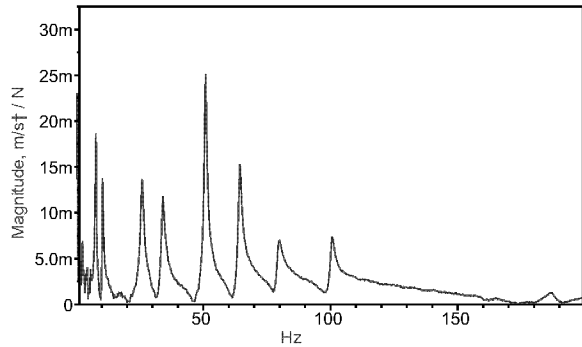


(b) Case II

Fig. 10. Measured transfer function in different cases.



(c) Case III



(d) Case IV

Fig. 10. (Continued)

influencing the model updating results. In the calculation process, the two factors can hardly be separated. If both types of errors are small or they compensate each other, sufficiently accurate identification can be achieved.

GAHA consists of GA and SAA. Unlike the traditional gradient-based optimization method, GA does not depend on the specified search direction. It randomly produces the new chromosomes in the whole solution space. Take Case IV as an example, four stories of concrete elastic modulus and three values of independent dynamic shear modulus of soil need to be identified according to the engineering experience. The search ranges are defined as:

$$E_1, E_2, E_3, E_4 \in [2 e10, 5 e10], \tag{15}$$

$$G_1, G_2, G_3 \in [2e7, 8e7]. \tag{16}$$

The objective functions are selected according to the following criterion<sup>9</sup>:

$$J_\omega = \sum_{i=1}^{N_f} W_{ai} \left( \frac{\omega_{mi} - \omega_{ai}}{\omega_{mi}} \right)^2, \tag{17}$$



$$J_\phi = \frac{1}{N_f} \sum_{i=1}^{N_f} W_{\phi_i} (\phi_{mi} - \phi_{ai})^T (\phi_{mi} - \phi_{ai}), \quad (18)$$

in which  $\omega_{mi}$  and  $\omega_{ai}$  are the  $i$ th measured frequency and analytical frequency, respectively;  $\phi_{mi}$  and  $\phi_{ai}$  are the  $i$ th measured modal shapes and analytical mode shapes, respectively,  $N_m$  is the number of selected modes,  $W_{ai}$  and  $W_{\phi_i}$  are the  $i$ th mode's weighting factors.  $W_{\phi_i}$  can be chosen as the reciprocal of averaged discrete errors in the mode shapes, as listed in Table 6.  $W_{ai}$  is set the same weighting factor as 0.25 from many time measurements. The optimization criterion, considering natural frequencies and mode shapes, is defined as

$$J_{\omega\phi} = W_1 J_\omega + W_2 J_\phi, \quad (19)$$

in which  $W_1$  and  $W_2$  are the participant factors of the natural frequencies and assembled participant factors of mode shapes.

In GA of GAHA, the initial population number is the amount of initial chromosomes. The evolutionary generation is the iteration number. By using the generation gap, the number of offspring is smaller than the number of parents.

In this paper, the Gray Code is used for encoding. The initial population number, evolutionary generation, and the generation gap are set as 100, 100, and 0.9, respectively. The random sample criterion is used as the selection method, and shuffling cards crossing is used as crossing method. The crossing probability is set as 0.7, and the mutation probability is set as 0.003.

In SA of GAHA, initial temperature is set as  $T = 50^\circ$ , based on the real coding method, the parallel searching mechanism is used in chromosome produced by GA in GAHA, the optimization scheme of producing status function is set as:

$$x(k+1) = x(k) + \eta \cdot x(k) \cdot \xi, \quad (20)$$

in which  $\eta$  is the disturbance parameter, taking from a normal distribution with the probability density function as:

$$f(\xi) = \frac{1}{\sqrt{2\pi}\sigma} \exp\left(\frac{-\xi^2}{2\sigma}\right), \quad (21)$$

in which  $\sigma$  means standard deviation. The annealing parameter is set as:

$$T = T_0(0.95)^{g-1}. \quad (22)$$

In general, GA may fall into local optimum, but SA easily produce large disturbance, so it may reach the global optimum.

Table 6. The weighting factor of different vibration shapes.

Weighting factor	$W_{\phi_1}$	$W_{\phi_2}$	$W_{\phi_3}$	$W_{\phi_4}$
Value	0.2553	0.3058	0.2267	0.2121

### 5.2. Parameter selection in SA

In GA of GAHA, parameter selection has been extensively researched. There are empirical value ranges that can be selected. However, in SA of GAHA, two important parameters have great influences on the operation velocity and the convergence of the results. In order to know whether the annealing process is sufficient or not, the annealing parameter  $g$  should be carefully selected. When the temperature control parameter is small enough, a high quality solution can be obtained. The value also has the relation with the computing time. The annealing parameters are selected as 20, 40, and 60.

Another parameter is the disturbance parameter  $\eta$ . If the parameter is too large, it will cause disturbance in a large range and leads to random search. If the value is too small, it will have no disturbance effect. The disturbance parameters are selected as 0.05, 0.03, and 0.01.

The annealing parameter value and disturbance parameter value are combined in parameter optimal selection. Take Case IV for example, three groups of numerical experiments are conducted. In Fig. 11, when  $g$  remains unchanged, the program converges fast with  $\eta = 0.01$ . Moreover, in Fig. 12, when  $\eta$  remains unchanged, the program converges fast with  $g = 20$ . Therefore in the following analysis,  $\eta$  and  $g$  are set as 0.01 and 20, respectively.

### 5.3. Physical parameter identification by GAHA and SA

Four cases of physical parameter identification are conducted. It is helpful to know the changes of elastic modulus of the concrete and dynamic shear modulus of the soil with increasing storey, which has important significance to long time health monitoring of the structure.

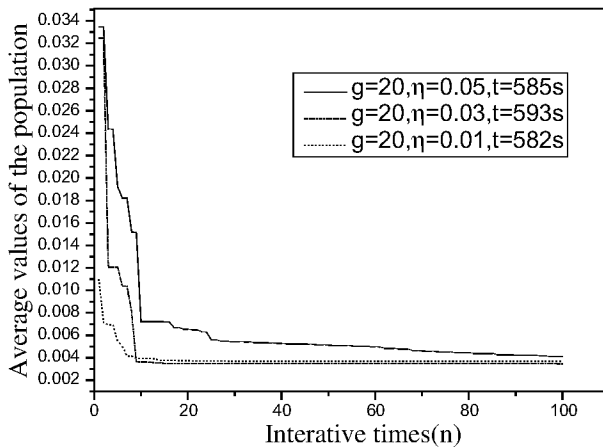


Fig. 11. The average value of population with the varies of  $\eta$ .

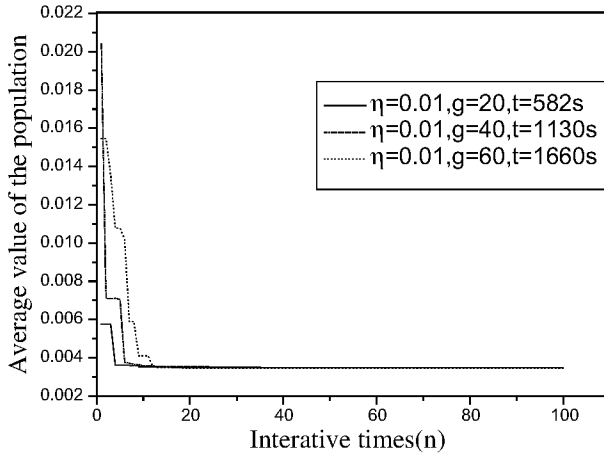


Fig. 12. The average value of population with the varies of  $g$ .

The elastic modulus of concrete and dynamic shear modulus of soil are identified with increasing number of storey and are presented in Table 7. Each storey’s elastic modulus of concrete increases with the number of storey, since the concrete strength increases with age. The dynamic shear modulus of soil foundation also increases with the storey (i.e with the upper structural weight). The values of three dynamic shear modulus of soil are close to each other. The regularity is in accordance with the reality.

The values of dynamic shear modulus by identification in Case I are close to the field experiment results. The identified values of elastic modulus of concrete are generally larger than that obtained from concrete compressive testing. There should be a relationship between the dynamic modulus and static modulus. For example, Ren and Roeck<sup>27</sup> regarded that the dynamic modulus is 12% larger than static modulus in concrete beam structures. Owing to the limitation of the experiment instrument, the dynamic elastic modulus of the concrete was not measured.

The identification results by SM are also shown in Table 8. The calculated natural frequencies by using identified modulus by SM and GAHA are presented in Table 9.

Table 7. The physical parameter identified by GAHA.

Modulus	Case I	Case II	Case III	Case IV
$E_1$	2.7845	3.2685	3.7520	3.7994
$E_2$	/	3.3956	3.6673	3.7984
$E_3$	/	/	3.5835	3.7246
$E_4$	/	/	/	3.6969
$G_1$	4.8752	5.3358	6.1928	6.2752
$G_2$	3.5271	5.3421	6.2921	6.9955
$G_3$	4.8246	5.4245	6.4383	6.1712

Unit: elastic modulus of concrete  $E \times 10^{10} \text{ N/m}^2$ ,  
dynamic shear modulus of soil  $G \times 10^7 \text{ N/m}^2$ .

Table 8. The physical parameter identified by SM.

Modulus	Case I	Case II	Case III	Case IV
$E_1$	2.5415	3.0159	3.6519	3.9886
$E_2$	/	3.4983	4.9146	4.6607
$E_3$	/	/	2.6850	4.0833
$E_4$	/	/	/	3.3983
$G_1$	6.9608	7.5252	7.6464	7.7155
$G_2$	6.9608	7.3175	7.5553	7.5553
$G_3$	6.9608	7.5252	7.6160	7.6848

Unit: elastic modulus of concrete  $E \times 10^{10} \text{ N/m}^2$ ,  
dynamic shear modulus of soil  $G \times 10^7 \text{ N/m}^2$ .

Table 9. The comparison of calculating and measuring modes.

Case	Order	Tested (Hz)	GAHA (Hz)	GAHA error (%)	SM (Hz)	SM error (%)
Case I	1st	20.1	20.1	0.00	20.1	0.00
Case II	1st	13.4	13.5	0.75	13.4	0.00
	2nd	51.2	50.9	-0.59	51.2	0.00
Case III	1st	9.9	10.4	5.05	10.7	8.08
	2nd	34.1	35.4	3.81	34.8	2.05
	3rd	69.3	68.2	-1.59	68.7	-0.87
Case IV	1st	7.7	8.2	6.49	8.7	12.99
	2nd	26.1	26.9	3.07	27.8	6.51
	3rd	50.6	50.8	0.40	52.2	3.16
	4th	79.3	77.0	-2.90	80.3	1.26

The measured and calculated mode shapes are compared in Fig. 13. It is shown that GAHA can effectively identify the elastic modulus of concrete and dynamic shear modulus of soil, and it has a robust global searching ability.

### 6. Conclusions

In this paper, GAHA is presented to identify the physical parameters in a concrete frame structure on elastic foundation with isolated independent footings. The main conclusions are summarized below:

- (1) Traditional SGA has a global-searching ability, but its efficiency could be influenced by the “premature problem” and “cheating problem.” SAA is another global searching method and it has good characters of local hill-climbing. GAHA combines the two algorithms in a series form so that the searching ability and hill-climbing ability are greatly improved.
- (2) Four cases of modal experiments were conducted on a four-storey concrete frame structure on elastic foundation where the number of storey is gradually increased. The measured natural frequencies and mode shapes were provided for the parameter identification by GAHA and SM.

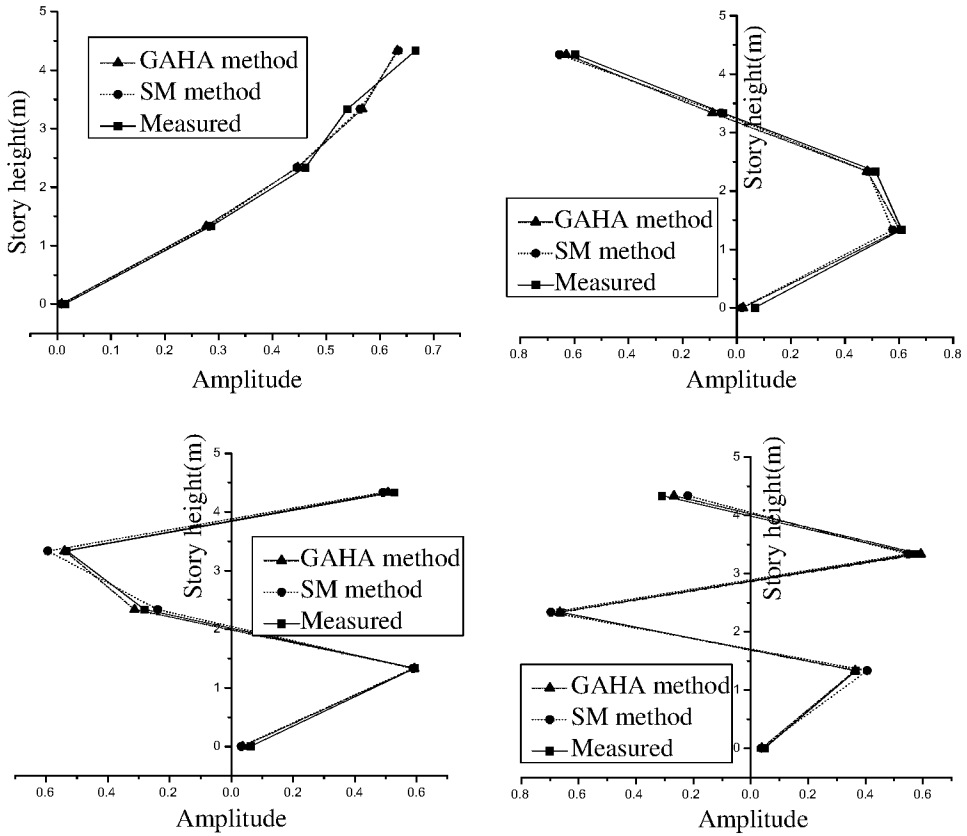


Fig. 13. Comparison of measured and calculated mode shapes (Case IV).

- (3) In GAHA, the annealing parameter  $g$  and disturbance parameter  $\eta$  have important influences on the searching efficiency and global searching ability. The two parameters were optimally selected by the numerical analysis.
- (4) For four cases of modal experiments, the results identified by GAHA are better than that by SM. All the elastic modulus of concrete and dynamic shear modulus of soil foundation are found to increase with the number of storey.

**Acknowledgments**

The authors are grateful for the financial support provided by the National Natural Science Foundation of China (NSFC) under Grant No. 50678064 and the Program for Changjiang Scholars and Innovative Research Team in University (PCSIRT) under Grant No. IRT0619.

**References**

1. M. I. Friswell and J. E. Mottershead, *Finite Element Model Updating in Structural Dynamics* (Kluwer Academic Publishers, Dordrecht, Netherlands, 1995).

2. S. W. Doebling, C. R. Farrar, M. B. Prime and D. W. Shevitz, Damage identification and health monitoring of structural and mechanical systems from changes in their vibration characteristics, *Report Los Alamos National Laboratory, Technical Report LA-13070-MS*, 1996.
3. S. W. Doebling, C. R. Farrar and M. B. Prime, A summary review of vibration-based damage model updating methods, *Shock Vib. Digest* **30**(2) (1998) 91–105.
4. R. V. Whitman, N. J. Protonotarios and F. M. Nelson, Case study of dynamic soil-structure interaction, *J. Soil Mech. Found. Div.* **99**(11) (1973) 997–1009.
5. H. L. Wong and M. D. Trifuriac, A comparison of soil-structure interaction calculations with results of full-scale forced vibration tests, *Soil Dynam. Earthquake Eng.* **7**(1) (1988) 22–31.
6. S. Hans, C. C. Boutin and E. Ibraim, In situ experiments and seismic analysis of existing buildings, Part I: Experimental investigations, *Earthquake Eng. Struct. Dynam.* **34**(12) (2005) 1513–1529.
7. A. C. Chassiakos, S. F. Masri, R. D. Nayeri, J. P. Caffrey, G. T. Zong and H. P. Chen, Use of vibration monitoring data to track structural changes in a retrofitted building, *Struct. Contr. Health Monit.* **14**(2) (2005) 218–238.
8. E. Luco and F. C. P. Barros, Identification of structural and soil properties from vibration tests of the Hualien containment model, *Earthquake Eng. Struct. Dynam.* **34**(1) (2005) 21–48.
9. M. I. Friswell, J. E. T. Penny and S. D. Garvey, A combined genetic and eigen-sensitivity algorithm for the location of damage in structures, *Comput. Struct.* **69**(5) (1998) 547–556.
10. W. J. Yi, and X. Liu, Damage diagnosis of structures by genetic algorithms, *Eng. Mech.* **18**(1) (2001) 64–71 (in Chinese).
11. H. Hao and Y. Xia, Vibration-based damage detection of structures by genetic algorithm, *J. Comput. Civil Eng.* **16**(2) (2002) 222–229.
12. F. T. K. Au, Y. S. Cheng, L. G. Tham and Z. Z. Bai, Structural damage detection based on a micro-genetic algorithm using incomplete and noisy modal test data, *J. Sound Vib.* **259**(5) (2003) 1081–1091.
13. Y. Lu and Z. G. Tu, Dynamic model updating using a combined genetic-eigensensitivity and application in seismic response prediction, *Earthquake Eng. Struct. Dynam.* **34**(9) (2005) 1149–1170.
14. R. Perera and R. Torres, Structural damage detection via modal data with genetic algorithms, *J. Struct. Eng.* **132**(9) (2006) 1491–1501.
15. M. J. Perry, C. G. Koh and Y. S. Choo, Modified genetic algorithm strategy for structural identification, *Comput. Struct.* **84**(8–9) (2006) 529–540.
16. B. Sahoo and D. Maity, Damage assessment of structures using hybrid neuro-genetic algorithm, *Appl. Soft Comput.* **7**(1) (2007) 89–104.
17. R. J. Balling, Optimal steel frame design by simulated annealing, *J. Struct. Eng.* **117**(6) (1991) 1780–1795.
18. R. L. Levin and N. A. J. Lieven, Dynamic finite element model updating using simulated annealing and genetic algorithms, *Mech. Syst. Signal Process.* **12**(1) (1998) 91–120.
19. S. R. Tzan and C. P. Pantelides, Annealing strategy for optimal structural design, *J. Struct. Eng.* **122**(7) (1996) 815–827.
20. R. S. He and S. F. Hwang, Identifying damage in spherical laminate shells by using a hybrid real-parameter genetic algorithm, *Composite Struct.* **80**(1) (2007) 32–41.
21. L. S. Kang, Y. Xie and S. Y. You, *Non Numerical Parallel Algorithm-Simulated Annealing Algorithm* (Science Press, Beijing, 1997) (in Chinese).
22. L. Wang, *Intelligent Optimization Algorithms with Applications* (Tsinghua University Press, Beijing, 2001) (in Chinese).

23. J. M. W. Brownjohn, P. Q. Xia, H. Hao and Y. Xia, Civil structure condition assessment by FE model updating: Methodology and case studies, *Finite Elem. Anal. Des.* **37**(10) (2001) 761–775.
24. X. J. Wang, *Dynamic Foundation and Basement* (Science Press, Beijing, 2001) (in Chinese).
25. National standard of the People's Republic of China, *Chinese Code for Design of Concrete Structures* (GB 50010-2002) (China Architecture & Building Press, Beijing, 2002).
26. A. Pais and E. Kausel, Approximate formulas for dynamic stiffness of rigid foundations, *Soil Dynam. Earthquake Eng.* **7**(2) (1988) 213–227.
27. W. X. Ren and G. D. Roeck, Structural damage identification using modal data II: Test verification, *J. Struct. Eng.* **128**(1) (2002) 96–104.